Article

Duplex-Promoted Platination of Adenine-N3 in the Minor Groove of DNA: Challenging a Longstanding Bioinorganic Paradigm

Colin G. Barry, Cynthia S. Day, and Ulrich Bierbach

J. Am. Chem. Soc., **2005**, 127 (4), 1160-1169• DOI: 10.1021/ja0451620 • Publication Date (Web): 07 January 2005

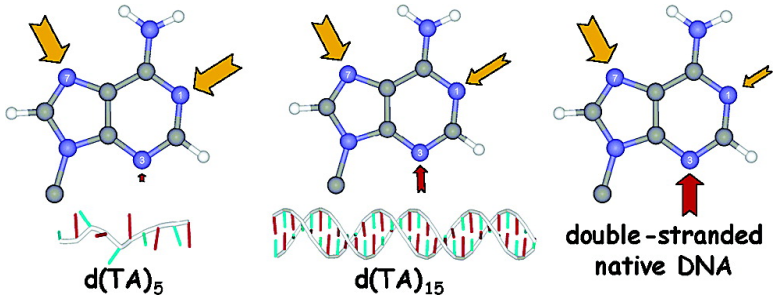

More About This Article

Additional resources and features associated with this article are available within the HTML version:

- Supporting Information
- Links to the 8 articles that cite this article, as of the time of this article download
- Access to high resolution figures
- Links to articles and content related to this article
- Copyright permission to reproduce figures and/or text from this article

View the Full Text HTML

J|A|C|S
ARTICLES
Published on Web 01/07/2005

Duplex-Promoted Platination of Adenine-N3 in the Minor Groove of DNA: Challenging a Longstanding Bioinorganic Paradigm

Colin G. Barry, Cynthia S. Day, and Ulrich Bierbach*

Contribution from the Department of Chemistry, Wake Forest University, P.O. Box 7486, Reynolda Station, Winston-Salem, North Carolina 27109

Received August 11, 2004; E-mail: bierbau@wfu.edu

Abstract: The interactions of [Pt(en)Cl(ACRAMTU-*S*)]$(NO_3)_2$ (PT-ACRAMTU, en = ethane-1,2-diamine, ACRAMTU = 1-[2-(acridin-9-ylamino)ethyl]-1,3-dimethylthiourea) with adenine in DNA have been studied using a combination of analytical and high-resolution structural methods. For the first time, a cytotoxic platinum(II) complex has been demonstrated to form adducts in the minor groove of DNA through platination of the adenine-N3 endocyclic nitrogen. An acidic depurination assay was developed that allowed the controlled and selective (pH 2, 60 °C, 12 h) release of platinum-modified adenine from drug-treated nucleic acid samples. From the digested mixtures, three adducts were isolated by semipreparative reverse phase high-performance liquid chromatography and studied by electrospray ionization mass spectrometry (in-line LC−MS), variable-pH ^{1}H NMR spectroscopy, and, where applicable, X-ray crystallography. The three species were identified as the N7 (**A*-I**), N3 (**A*-II**), and N1 (**A*-III**) linkage isomers of [Pt(en)(ACRAMTU-*S*)(adenine)]$^{3+}$ (**A***). Incubations carried out with the single- and double-stranded model sequences, $d(TA)_5$ and $d(TA)_{15}$, as well as native DNA indicate that the adduct profiles (**A*-I**:**A*-II**:**A*-III** ratios) are sensitive to the nature of the nucleic acid template. **A*-II** was found to be a double-strand specific adduct. The crystal structure of this adduct has been determined, providing ultimate evidence for the N3 connectivity of platinum. **A*-II** crystallizes in the triclinic space group $P\bar{1}$ in the form of centrosymmetric dimers, $\{[Pt(en)(ACRAMTU\text{-}S)(adenine\text{-}N3)]_2\}^{6+}$. The cations are stabilized by a combination of adenine−adenine base pairing (N6···N1 2.945(5) Å) and mutual acridine−adenine base stacking. Tandem mass spectra and ^{1}H chemical shift anomalies indicate that this type of self-association is not merely a crystal packing effect but persists in solution. The monofunctional platination of adenine at its N7, N3, and N1 positions in a significant fraction of adducts breaks a longstanding paradigm in platinum−DNA chemistry, the requirement for nucleophilic attack of guanine-N7 as the principal step in cross-link formation. The biological consequences and potential therapeutic applications of the unique base and groove recognition of PT-ACRAMTU are discussed.

Introduction

Genomic DNA and the proteins and enzymes involved in its replication, transcription, and repair are targets for cancer therapy. Many antineoplastic drugs cause cancer cell death by irreparably damaging DNA in the cell's nucleus.[1] Despite their notorious lack of cancer cell specificity, DNA-targeted agents continue to play an important role in the clinical management of malignancies worldwide.[2] In addition to their indiscriminate reactivity, reflected in the fact that the most effective therapies have significant side effects, small-molecule anticancer agents often show an inherent lack of DNA sequence selectivity. The cytotoxic effect of DNA binders is mediated by enzymes and proteins, which act on DNA in a sequence- and/or groove-specific manner. Thus, the design of new agents recognizing DNA sequence and DNA secondary structure more selectively is one of the high priority goals in anticancer drug development.[3]

Platinum-based therapeutics, including the historical complex *cis*-diamminedichloroplatinum(II) (cisplatin, Chart 1) and its congeners, are a class of agents that are being widely explored as treatments for solid tumors.[4] The cytotoxic effect of cisplatin is believed to ultimately result from cross-links formed by the *cis*-$[Pt(NH_3)_2]^{2+}$ fragment in DNA sequences containing adjacent purine bases. The majority of bifunctional adducts formed by this drug are 1,2 intrastrand cross-links in GG (major) and 5′-AG (minor) sequences (G = guanine, A = adenine), in which platinum forms coordinative bonds with the nucleophilic N7 positions of the nucleobases in the major groove of the biopolymer.[5] The first binding step in the formation of these adducts involves platination of guanine-N7 by the mono- or diaqua form

(1) Baguley, B. C. In *Anticancer Drug Development*; Baguley, B. C., Kerr, D. J., Eds.; Academic Press: San Diego, CA, 2002; pp 1−11.
(2) Sikora, K.; Advani, S.; Koroltchouk, V.; Magrath, I.; Levy, L.; Pinedo, H.; Schwartsmann, G.; Tattersall, M.; Yan, S. *Ann. Oncol.* **1999**, *10*, 385−390.
(3) Hurley, L. H. *Nat. Rev. Cancer* **2002**, *2*, 188−200.
(4) Reedijk, J. *Proc. Natl. Acad. Sci. U.S.A.* **2003**, *100*, 3611−3616.
(5) Gelasco, A.; Lippard, S. J. In *Topics in Biological Inorganic Chemistry*; Clarke, M. J., Sadler, P. J., Eds.; Springer: New York, 1999; Vol. I, pp 1−43.

10.1021/ja0451620 CCC: $30.25

Chart 1

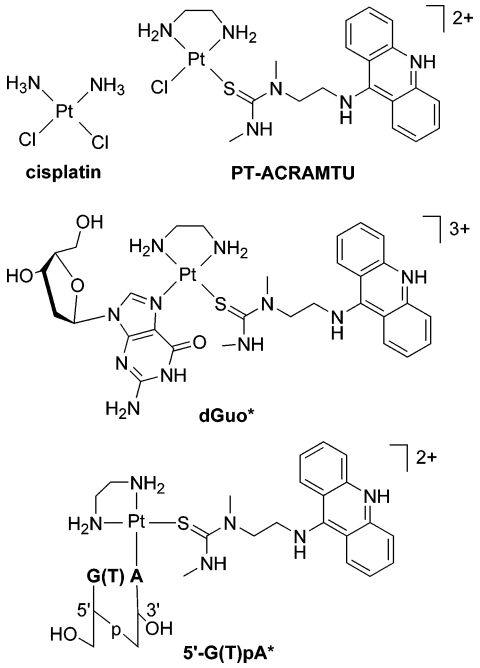

of the drug, which is favored over adenine-N7 binding, followed by closure to the G-N7/G-N7 and A-N7/G-N7 bifunctional chelates.[6] Recognition of guanine-rich DNA sequences by aquated cisplatin is driven by simple electrostatics, and binding occurs without noticeable long-range sequence specificity.[7]

The natural high selectivity of platinum(II) for guanine-N7 in the DNA's major groove is a common feature of all therapeutically active second- and third-generation cisplatin derivatives.[8] Essentially, the same base preference is observed for nonclassical platinum drugs, including multinuclear complexes[9] and complexes exhibiting trans geometry;[10] guanine-N7 is the primary target, although the types of adducts formed by these agents are distinctly different from those induced by the clinical complexes. The design of the nonclassical agents was motivated by the hypothesis that the biological properties of platinum can be tuned at the DNA adduct level, which would ultimately lead to an altered spectrum of antitumor activity. Following this concept, we have developed a new type of platinum−intercalator conjugate by tethering a monofunctional platinum moiety to the minor-groove-oriented side chain of the novel 9-aminoacridine derivative, 1-[2-(acridin-9-ylamino)ethyl]-1,3-dimethylthiourea (ACRAMTU).[11] [Pt(en)Cl(ACRAMTU-*S*)]-$(NO_3)_2$ (PT-ACRAMTU, en = ethane-1,2-diamine; Chart 1) was developed to explore the possibility of producing useful antitumor activity through adducts other than the common cross-links in runs of purine bases. (PT-ACRAMTU and several of its derivatives, indeed, show promising activity in various solid tumor cell lines.[11−13]) In particular, we were interested in

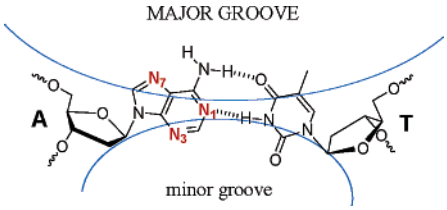

Figure 1. Structure of the Watson−Crick AT pair with potential sites of platination highlighted in red. The blue lines indicate the DNA grooves.

generating a pharmacophore in which the intercalating moiety would dictate the groove and sequence specificity of platinum binding. In previous studies, we employed a wide range of physical and biochemical methods to shed light on the DNA binding of PT-ACRAMTU. The most striking feature of this conjugate, which binds through a dual mechanism involving intercalation and monofunctional platination of nucleobase nitrogen,[14,15] was its tendency to induce covalent DNA damage at the preferred intercalation sites of ACRAMTU: adduction occurs with guanine (~80%) and adenine (~20%) in the sequences 5′-CG/CG, 5′-TA/TA, and 5′-GA/TC.[16,17] In essence, we demonstrated that a relatively simple chemical modification, namely, replacement of one chloro leaving group in classical $[PtCl_2(en)]$ with ACRAMTU, leads to a dramatic loss of guanine specificity of platinum and a DNA adduct profile complementary to that of cisplatin.[18] While we were able to unequivocally establish N7 as the (expected) site of platination in dGuo*[19] (Chart 1; dGuo = 2′-deoxyguanosine; the asterisk denotes the $[Pt(en)(ACRAMTU)]^{3+}$ fragment), no high-resolution data were available for the unusual adenine-containing fragments, 5′-G(T)pA*[17] (Chart 1), isolated from enzymatic digests. On the basis of circumstantial biochemical evidence, we argued that N3 might be a likely platinum binding site.[17,18]

Considering the presence of multiple potential sites of platination in adenine, the elucidation of the adenine-binding profile in a complex biopolymer at atomic resolution is not a trivial task. Here, we demonstrate for the first time using a newly developed base-selective depurination assay and a combination of analytical and high-resolution structural methods the ability of platinum(II) to covalently modify adenine in double-stranded DNA at its endocyclic nitrogen N3, which is located in the minor groove (Figure 1). This adduct, which was isolated along with the more common N1 and N7 isomers as platinum-modified free purine bases, is unprecedented in platinum antitumor chemistry and has been previously observed only in model systems and chemically modified adenines.[20−22] The duplex-specific formation of the adenine-N3 adduct renders the minor groove of DNA and proteins that recognize and bind to it a new potential target for platinum-based chemotherapy.

(6) Davies, M. S.; Berners-Price, S. J.; Hambley, T. W. *J. Am. Chem. Soc.* **1998**, *120*, 11380−11390.
(7) Burstyn, J. N.; Heiger-Bernays, W. J.; Cohen, S. M.; Lippard, S. J. *Nucleic Acids Res.* **2000**, *28*, 4237−4243.
(8) Wong, E.; Giandomenico, C. M. *Chem. Rev.* **1999**, *99*, 2451−2466.
(9) Farrell, N.; Qu, Y.; Roberts, J. D. In *Topics in Biological Inorganic Chemistry*; Clarke, M. J., Sadler, P. J., Eds.; Springer: New York, 1999; Vol. I, pp 99−115.
(10) Farrell, N. *Met. Ions Biol. Syst.* **1996**, *32*, 603−639.
(11) Martins, E. T.; Baruah, H.; Kramarczyk, J.; Saluta, G.; Day, C. S.; Kucera, G. L.; Bierbach, U. *J. Med. Chem.* **2001**, *44*, 4492−4496.
(12) Ackley, M. C.; Barry, C. G.; Allen, A. M.; Farmer, M. C.; Springer, B.-E.; Day, C. S.; Wright, M. W.; Berners-Price, S. J.; Hess, S. M.; Bierbach, U. *J. Biol. Inorg. Chem.* **2004**, *9*, 453−461.
(13) Hess, S. M.; Mounce, A. M.; Sequeira, R. C.; Augustus, T. M.; Ackley, M. C.; Bierbach, U. *Cancer Chemother. Pharmacol.* In press.
(14) Baruah, H.; Rector, C. L.; Monnier, S. M.; Bierbach, U. *Biochem. Pharmacol.* **2002**, *64*, 191−200.
(15) Baruah, H.; Bierbach, U. *J. Biol. Inorg. Chem.* **2004**, *9*, 335−344.
(16) Baruah, H.; Bierbach, U. *Nucleic Acids Res.* **2003**, *31*, 4138−4146.
(17) Barry, C. G.; Baruah, H.; Bierbach, U. *J. Am. Chem. Soc.* **2003**, *125*, 9629−9637.
(18) Budiman, M. E.; Alexander, R. W.; Bierbach, U. *Biochemistry* **2004**, *43*, 8560−8567.
(19) Baruah, H.; Day, C. S.; Wright, M. W.; Bierbach, U. *J. Am. Chem. Soc.* **2004**, *126*, 4492−4493.

Experimental Section

Materials. [Pt(en)(ACRAMTU-*S*)Cl](NO$_3$)$_2$ (PT-ACRAMTU; en = ethane-1,2-diamine; ACRAMTU = 1-[2-(acridin-9-ylamino)ethyl]-1,3-dimethylthiourea, acridinium cation) was synthesized according to the published procedure and isolated as its methanol monosolvate.[11] Stock solutions of PT-ACRAMTU in the appropriate buffers were prepared immediately before the incubations and stored at −20 °C. 2′-Deoxyadenosine (dAdo) and calf thymus DNA were purchased from Sigma. Calf thymus DNA was dissolved in 10 mM Tris buffer (pH 7.1) containing 100 mM NaCl and purified by dialysis against buffer using 6−8 kDa molecular weight cutoff (MWCO) dialysis tubing. The purity of the DNA was assessed spectrophotometrically from the ratio of absorbances at 260 and 280 nm.[23] The 10mer and 30mer alternating sequences, d(TA)$_5$ and d(TA)$_{15}$, were synthesized using phosphoramidite chemistry and desalted by Integrated DNA Technologies Inc. (Coralville, IA). Nucleic acids were annealed, where appropriate, by slowly cooling buffered solutions from 90 °C to room temperature. DNA concentrations were determined from absorbances at 260 nm using Beer's law with ϵ_{260} (calf thymus) = 12 824 M^{-1} cm^{-1},[24] ϵ_{260} (d(TA)$_5$) = 11 180 M^{-1} cm^{-1}, and ϵ_{260} (d(TA)$_{15}$) = 11 093 M^{-1} cm^{-1}. Buffers were prepared from biochemical-grade chemicals (Fisher/Acros) and 0.22 μM-filtered DNase/RNase-free water from a Milli-Q A10 synthesis water purification system. HPLC grade solvents were used in all chromatographic separations. All other chemicals and solvents were purchased from common vendors and used as supplied.

Incubations and Acidic Digestion. All incubations were performed in 10 mM Tris buffer/100 mM NaCl (pH 7.1). Reactions of PT-ACRAMTU with calf thymus DNA were performed in the dark for 18 h at 37 °C at drug-to-nucleotide incubation ratios (r_f) of 0.1, 0.2, and 0.4. Large-scale reactions between PT-ACRAMTU and calf thymus DNA were conducted by incubating 100 mg of purified native DNA in 1.0 L of buffer. With constant stirring, 77 mg (0.1 mmol) of PT-ACRAMTU in 25 mL of buffer were added dropwise, and the mixture was incubated in the dark for 15 h at 37 °C. The solution was reduced to a volume of approximately 200 mL (rotary evaporation, ≤40 °C) and exhaustively dialyzed against Millipore water using 6−8 kDa MWCO dialysis tubing. Reactions of PT-ACRAMTU with 2′-deoxyadenosine (dAdo) were conducted with 5.0 mg (2.0×10^{-5} mol) of nucleoside and 13.3 mg (1.8×10^{-5} mol) of PT-ACRAMTU in 1.5 mL of buffer. The solution was mixed thoroughly and incubated in the dark for 18 h at 37 °C. Acidic digestions were performed by adjusting the pH of the reaction mixtures to 2 using formic acid and heating at 60 °C for 12 h in the dark. Undigested native DNA was removed by centrifugal filtration at 14 000 rpm at 4 °C for several hours using Microcon YM-3 spin tubes (Millipore, Billerica, MA). After digestion, chromatographic separations of the resulting adduct mixtures were carried out by analytical or semipreparative HPLC as described below. In the time-course experiments, PT-ACRAMTU was incubated with d(TA)$_{15}$ at $c_{Pt} = 6.0 \times 10^{-5}$ M and $c_{oligo} = 2.0 \times 10^{-4}$ M. Incubations and subsequent acidic digestions were performed using the above protocols. From the acidified mixtures, 100 μL aliquots were removed at time points of 0, 1, 2, 3, 6, and 12 h, quenched in liquid nitrogen, stored at −20 °C, and subjected to in-line HPLC/mass spectrometry (LC−MS) analysis as described below.

Chromatographic Separations. HPLC separations of the product mixtures resulting from incubations of PT-ACRAMTU with calf thymus DNA were performed on a LaChrom Hitachi D-7000 system equipped with an L-7420 UV−visible variable-wavelength detector and a fraction collector. Semipreparative separations were performed using an Agilent Zorbax SB-C18 reverse phase column (250 × 9.4 mm/5 μm). *Eluents*: solvent A = 25 mM citric acid, pH 5.4; solvent B = MeOH. *Gradient*: 79% A/21% B → 75% A/25% B in 0−27 min. *Flow rate*: 2.7 mL/min (referred to as HPLC protocol A). Analytical separations of adducts in acidic digestion mixtures were performed using the above system or the HPLC module of an Agilent Technologies 1100LS/MSD Trap instrument equipped with a multiwavelength diode-array detector and a thermostated autosampler. *Column*: Agilent Zorbax SB-C18 reverse phase 150 × 4.6 mm/5 μm, T = 25 °C (for 1100LS system). *Eluents*: solvent A = 0.1% formic acid in water; solvent B = 0.1% formic acid in acetonitrile. *Gradient*: 95% A/5% B → 81% A/19% B in 0−28 min. *Flow rate*: 0.5 mL/min (referred to as HPLC protocol B). Elution of PT-ACRAMTU-modified adenine in both semipreparative and analytical separations was monitored at 254 and 413 nm. The pH of the combined fractions of each adduct was adjusted to 7.0 using 0.1 M NaOH. Approximately 2−5 mg of each adduct (**A*-I**, **A*-II**, and **A*-III**) were collected (quantified spectrophotometrically[14] with ϵ_{413} = 9450 M^{-1} cm^{-1}). To reduce the salt content (sodium chloride, sodium citrate), the samples were evaporated to dryness and the adducts extracted from the residue with methanol. The organic solvent was removed in vacuum, and the solid was redissolved in Millipore water and lyophilized twice. Each fraction was re-examined by LC−MS for purity.

Mass Spectrometry. Mass spectra were acquired on an Agilent Technologies 1100 LC/MSD ion trap mass spectrometer equipped with an atmospheric pressure electrospray ionization source. Adducts were introduced into the ionization source after passing though the in-line HPLC system using the chromatographic method described above with the eluent from 0 to 4 min diverted into the waste. Eluent nebulization was achieved with a N_2 pressure of 60 psi, and solvent evaporation was assisted by a flow of N_2 drying gas (300 °C, 11 L/min). Mass spectra were recorded with enhanced scan resolution (m/z 5500 s^{-1}) in positive ion mode over a m/z 190−1500 range. A capillary voltage of 1.8 kV was applied. Tandem mass spectra (MS/MS) of the ions of interest were generated by collision-induced dissociation (CID) of the trapped precursor ions using He as the collision gas. Solvent evaporation was assisted by a flow of N_2 drying gas (325 °C, 11 L/min). MS/MS spectra were acquired with a fragmentation amplitude of 1.2 V, a fragmentation cutoff of m/z 401, and an isolation width of m/z 4.0. All data were analyzed using the Agilent LC/MSD Trap Control 4.9 data analysis software.

NMR Spectroscopy. ^{1}H NMR (500 MHz) spectra were recorded on a Bruker DRX-500 instrument equipped with a 5 mm inverse three-channel Z-gradient probe and a variable-temperature unit. All spectra were acquired at 25 °C with a spectral width of 10 331 Hz, 65 536 data points, 16 transients, and a recycle delay of 1 s. Data sets were apodized using exponential multiplication and a line broadening of 0.3 Hz. ^{1}H chemical shifts were referenced to the most upfield signal of internal 3-(trimethylsilyl)-1-propanesulfonic acid sodium salt (DSS). Variable-pH ^{1}H NMR spectra of D_2O solutions were recorded in the pH range of 0−10. The pH was adjusted with 0.10, 1.0, and 5.0 M DCl and NaOD solutions and measured in the NMR tube using an Accumet micro combination electrode with calomel reference connected to an Orion 210A-plus pH meter. Solutions were titrated from high to low pH and finally back to neutral pH to demonstrate that the samples were chemically unchanged. Reported pH* values are uncorrected pH meter readings of the D_2O solutions.

X-ray Crystallography. Single crystals of **A*-I** and **A*-II** were grown by slow evaporation of sitting drops (17.5 μL) of aqueous solutions of the adducts at 4 °C over 7−10 days. To establish the optimal pH for crystal growth, 96-well MicroBatch high-throughput crystallization plates (Hampton Research, Aliso Viejo, CA) were used.

(20) Liu, Y.; Vinje, J.; Pacifico, C.; Natile, G.; Sletten, E. *J. Am. Chem. Soc.* **2002**, *124*, 12854−12862.
(21) Meiser, C.; Song, B.; Freisinger, E.; Peilert, M.; Sigel, H.; Lippert, B. *Chem.—Eur. J.* **1997**, *2*, 388−398.
(22) Amantia, D.; Price, C.; Shipman, M. A.; Elsegood, M. R. J.; Clegg, W.; Houlton, A. *Inorg. Chem.* **2003**, *42*, 3047−3056.
(23) Turner, P. C.; McLennan, A. G.; Bates, A. D.; White, M. R. H. *Instant Notes in Molecular Biology*; Bios Scientific Publishers: Oxford, U.K., 1997; pp 40−41.
(24) Fox, K. R. In *Drug−DNA Interaction Protocols*; Fox, K. R., Ed.; Humana Press: Totowa, NJ, 1997; pp 1−22.

Table 1. Crystal Data and Structure Refinement for [Pt(en)(ACRAMTU)(adenine-N3)]$(NO_3)_3 \cdot 5H_2O$ ([**A*-II**]$(NO_3)_3 \cdot 5H_2O$)

empirical formula	$C_{25}H_{44}N_{14}O_{14}PtS$[a]
formula weight	991.89 (including solvent)
T, K	213
wavelength, Å	0.71073
cryst syst, space group	triclinic, $P\bar{1}$
a, Å	10.307(1)
b, Å	13.307(1)
c, Å	15.129(1)
α, deg	78.244(1)
β, deg	82.033(1)
γ, deg	70.672(1)
V, Å^3	1911.2(2)
Z	2
D(calc), g cm^{-3}	1.724
μ, mm^{-1}	3.81
crystal size, color, habit	0.412 × 0.108 × 0.058 mm, pale yellow plates
abs corr	multiscan SADABS
final *R* indices[b] [$I > 2\sigma(I)$]	$R1 = 0.0429$, $wR2 = 0.1034$
R indices (all data)	$R1 = 0.0521$, $wR2 = 0.1080$

[a] For alternate formula due to anion/solvent disorder, see Supporting Information. [b] $R1 = \Sigma||F_o| - |F_c||/\Sigma|F_o|$; $wR2 = [\Sigma[w(F_o^2 - F_c^2)^2]/\Sigma w(F_o^2)^2]^{1/2}$.

Crystals of **A*-I** and **A*-II** were obtained at pH 4.2 and 6.2 (adjusted with HNO_3 and NaOH), respectively. The X-ray intensity data were measured on a Bruker SMART APEX CCD area detector system. The structures were solved and refined using the Bruker SHELXTL software package (version 6.12). Crystallographic data for [**A*-II**]$(NO_3)_3 \cdot 5H_2O$ and [**A*-I**]$(NO_3)_3 \cdot 4H_2O$ are summarized in Table 1 and Table S1 of the Supporting Information, respectively. Details of the structure determinations are supplied in CIF format as Supporting Information.

Results

Assay Design. The goal of this work was to explore the adenine-specific interactions of PT-ACRAMTU in double-stranded DNA at the atomic level. Previous analytical assays[17] used mixtures of single-strand and double-strand specific endonucleases and alkaline phosphatase to degrade native DNA modified with PT-ACRAMTU. The reproducibility of the adduct profiles in these assays critically depended on the batch quality of the enzymes and the protocol used. Furthermore, the structures of the modified DNA fragments isolated (see Chart 1) indicated that the efficiency of digestion depended on the nature of the individual adducts. Most importantly, enzymatic digestion proved to be not a viable method for generating the minor adenine adducts on a semipreparative scale. We therefore developed an assay based on chemical digestion that allowed the controlled release of modified adenine base from drug-treated DNA samples. The assay was inspired by earlier reports demonstrating that metal-modified adenine undergoes facile depurination in acidic media while the release of guanine complex was significantly retarded under the same conditions.[25,26] We exploited this difference in reactivity, which is a consequence of the distinctly different proton affinities of the platinated purine bases,[27] to selectively liberate platinum-modified adenine from the DNA (Figure 2). Briefly, calf thymus DNA, the single-stranded sequence d(TA)$_5$, double-stranded d(TA)$_{15}$, and 2′-deoxyadenosine (dAdo) were incubated with PT-ACRAMTU at neutral pH for 18 h at 37 °C according to

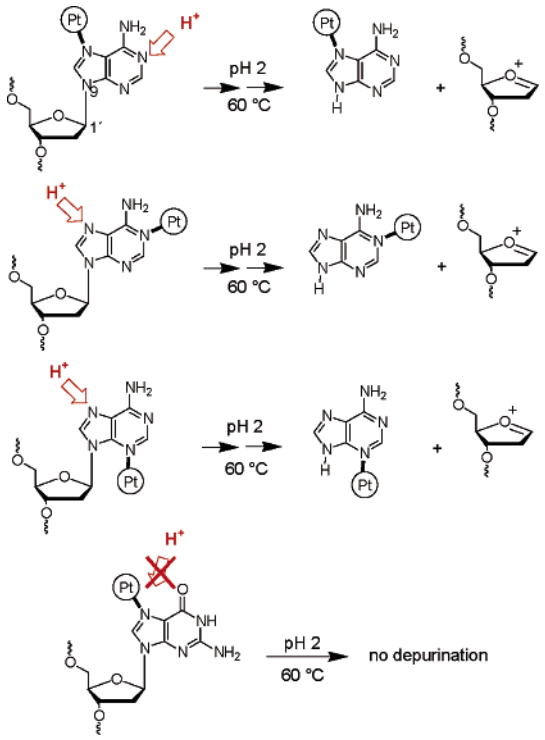

Figure 2. Acid-promoted heterolytic cleavage of the C1′−N9 glycosidic bond resulting in the selective release of platinum-modified adenine base. Partial protonation of adenine is possible regardless of the site of attachment of platinum, whereas protonation of guanine is prohibited due to selective binding of the metal to the N7 position, the only proton-affinic site in this nucleobase at pH 2 (ref 27).

conditions established in previous work.[17,18] The single- and double-stranded oligomers were included to study the effect of DNA secondary structure on adduct formation. The solutions were then adjusted to pH 2 and heated for 12 h at 60 °C to release modified adenine base (see Experimental Section for details). The resulting mixtures were analyzed and separated by reverse phase high-performance liquid chromatography (HPLC) and the adducts characterized by electrospray ionization mass spectrometry (ESI-MS), (variable-pH) ^{1}H NMR spectroscopy, and, where applicable, X-ray crystallography. Control experiments were performed to assess the stability of the isolated adducts under the conditions of the assay. It was verified that the adduct distribution observed is representative of the actual adduct profile in the DNAs prior to digestion: neither migration of platinum between endocyclic nitrogens (isomerization) nor dissociation of ligands from platinum was observed at pH 2 and elevated temperatures.

Detection and Identification of Adducts. To establish conditions for the controlled depurination of drug-modified DNA and (oligo)nucleotides, samples were removed at various time points from digestion mixtures of modified d(TA)$_{15}$, immediately frozen, or directly injected onto the HPLC column. (The time-consuming separation by centrifugal filtration of modified adenine adducts from polymeric debris in mixtures containing calf thymus DNA did not allow "real-time" HPLC monitoring of the adduct release from native DNA.) HPLC traces were recorded at an acridine-specific wavelength (413 nm). The time course of release of adducts is presented in Figure 3. Three peaks

(25) Iverson, B. L.; Dervan, P. B. *Nucleic Acids Res.* **1987**, *15*, 7823−7830.
(26) Arpalahti, J.; Käppi, R.; Hovinen, J.; Lönnberg, H.; Chattopadhyaya, J. *Tetrahedron* **1989**, *45*, 3945−3954.
(27) Griesser, R.; Kampf, G.; Kapinos, L. E.; Komeda, S.; Lippert, B.; Reedijk, J.; Sigel, H. *Inorg. Chem.* **2003**, *42*, 32−41.

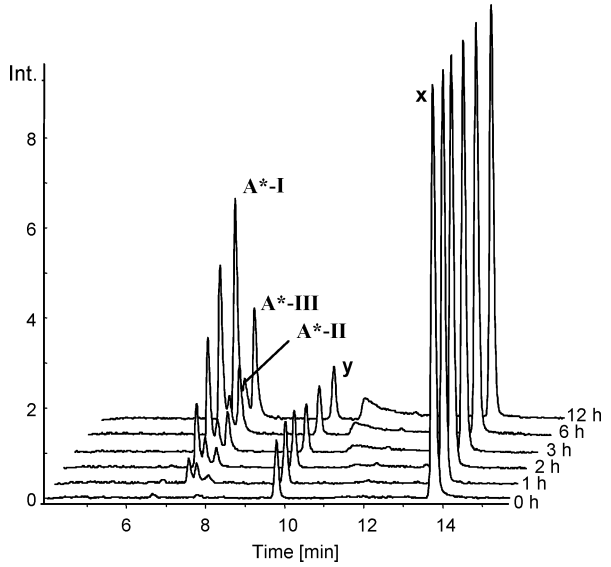

Figure 3. Depurination of platinated $d(TA)_{15}$ monitored by reverse phase HPLC (protocol A, see Experimental Section) using UV−visible detection at 413 nm. The three acridine-containing adducts, **A*-I**, **A*-II**, and **A*-III**, elute at retention times of 7.4, 7.7, and 7.9 min, respectively. The peaks of constant height were assigned to unreacted PT-ACRAMTU (x) and its hydrolyzed form, $[Pt(en)(H_2O)(ACRAMTU)]^{3+}$ (y), based on coelution of drug standards and mass spectral data.

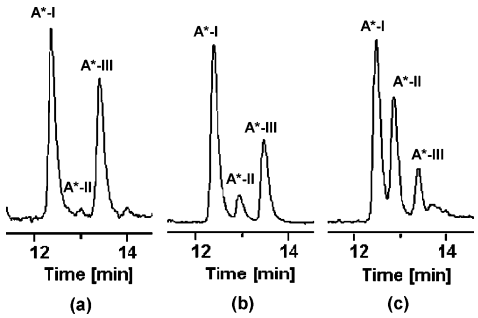

Figure 4. HPLC traces recorded at 413 nm of mixtures of the platinum-modified nucleic acids after 18 h of acidic digestion (separations were done using HPLC protocol B, see Experimental Section). Sequences and adduct distributions: (a) $d(TA)_5$ **A*-I**, 56%; **A*-II**, 1%; **A*-III**, 43%; (b) $d(TA)_{15}$ **A*-I**, 64%; **A*-II**, 7%; **A*-III**, 29%; (c) calf thymus DNA **A*-I**, 56%; **A*-II**, 33%; **A*-III**, 11%.

of increasing intensity, labeled **A*-I**, **A*-II**, and **A*-III**, are observed in the chromatograms recorded after 0, 1, 2, 3, 6, and 12 h of continuous digestion. Inspection of the peak integrals confirmed that the reaction was virtually complete after 12 h with adduct **A*-II** being released most rapidly, followed by **A*-I** and **A*-III**. The relative abundance of each adduct in the mixtures varied significantly with the nature of the nucleic acid template. In digested mixtures of single-stranded $d(TA)_5$ (Figure 4a) and dAdo (not shown), the two major adducts are **A*-I** and **A*-III** while **A*-II** is barely detectable. In double-stranded $d(TA)_{15}$ (Figure 4b), a significantly increased amount of **A*-II** and decreased amount of **A*-III** is observed compared to the single-stranded 10mer. (Thermal melting curves and CD spectra (Supporting Information) were recorded of the two synthetic alternating sequences, confirming that only $d(TA)_{15}$ existed in its double-stranded B-form[28] under the conditions used in incubations with PT-ACRAMTU.) An even more dramatic change in relative amounts of adducts was found for calf thymus DNA (Figure 4c), in which **A*-II** becomes the second most abundant and **A*-III** the least abundant adduct.

Electrospray ionization mass spectra of **A*-I**, **A*-II**, and **A*-III** were recorded for both the adduct mixtures and the isolated adducts using an in-line LC−MS setup. The data unequivocally demonstrate that the three species released in this digestion assay are isomers of the monofunctional platinum−adenine adduct, $[Pt(en)(adenine)(ACRAMTU)]^{3+}$ (**A***, M_r = 715.3). As could be expected, the UV−visible and mass spectra of the three species are virtually indistinguishable (Figure 5). Mass spectra recorded in positive-ion mode show a major peak at *m*/*z* 713, assigned to the $[A^*-2H]^+$ ions, as well as characteristic fragment ions produced by collisionally activated dissociation (CAD). These include fragments resulting from loss of bidentate en (*m*/*z* 653), loss of adenine base (*m*/*z* 578), and dissociation of the Pt−S bond (*m*/*z* 388 and 326) (Figure 5). On the basis of the UV−visible traces and mass spectra alone, it is impossible to discern the connectivity within the adducts, that is, the exact sites of platinum coordination. However, preliminary assignments were made at this point, which were confirmed by high-resolution techniques (vide infra), based on the following considerations. (i) At the nucleoside/tide level, platinum(II) complexes usually exhibit dual high affinity for adenine-N1 and adenine-N7.[29,30] In double-stranded DNA, adenine-N1 can be expected to be disfavored as a target site due to involvement in Watson−Crick hydrogen bonding with complementary thymine (Figure 1). The major adduct in the HPLC profiles in Figure 4 (**A*-I**) and adduct **A*-III**, which is less abundant in the double-stranded DNAs, were therefore assigned to the adenine-N7 and adenine-N1 adducts, respectively (Chart 2). This assignment is also supported by the relative rates of depurination in acidic media, where **A*-I** was released more readily.[26] (ii) In contrast to **A*-III**, **A*-II** appears to be a double-strand specific (and in agreement with our design rationale, intercalator-driven) adduct, which at this stage of the study was tentatively assigned to the adenine-N3 linkage isomer (Chart 2).

High-Resolution Structural Characterization of the Adducts. From the digested samples of platinum-treated calf thymus DNA, 2−5 mg of each adduct was collected using semipreparative HPLC separations. High-field ^{1}H NMR spectroscopy was used to provide evidence for the structures and the platinum connectivities proposed in Chart 2. The downfield regions in spectra recorded of pH*-adjusted D_2O solutions of **A*-I**, **A*-II**, and **A*-III** show the expected set of aromatic acridine protons, H1−H8, and the two nonexchangeable adenine protons, H2 and H8 (Figure 6, Table 2). At pH* 6.2, significant differences in chemical shifts are observed between the three adducts. In particular, $H2_{Ade}$ and $H8_{Ade}$ in adducts **A*-I** and **A*-II** appear significantly upfield shifted compared to the signals in free adenine. The opposite effect is usually observed for platinum binding to ring nitrogen adjacent to H2 and H8.[31] This chemical shift anomaly is the result of ring current effects[32] produced by the acridine chromophores in the adducts, which exist as self-stacked dimers both in solution and in the solid

(28) Gray, D. M.; Ratliff, R. L.; Vaughan, M. R. *Methods Enzymol.* **1992**, *211*, 389−406.
(29) Martin, R. B. *Met. Ions Biol. Syst.* **1996**, *32*, 61−89.
(30) Kampf, G.; Lüth, M. S.; Kapinos, L. E.; Müller, J.; Holý, A.; Lippert, B.; Sigel, H. *Chem.—Eur. J.* **2001**, *7*, 1899−1908.
(31) Sletten, E.; Frøystein, N. Å. *Met. Ions Biol. Syst.* **1996**, *32*, 397−418.
(32) Wilson, W. D.; Li, Y.; Veal, J. M. In *Advances in DNA Sequence Specific Agents*; Hurley, L. H., Ed.; JAI Press: New York, 1992; pp 89−165.

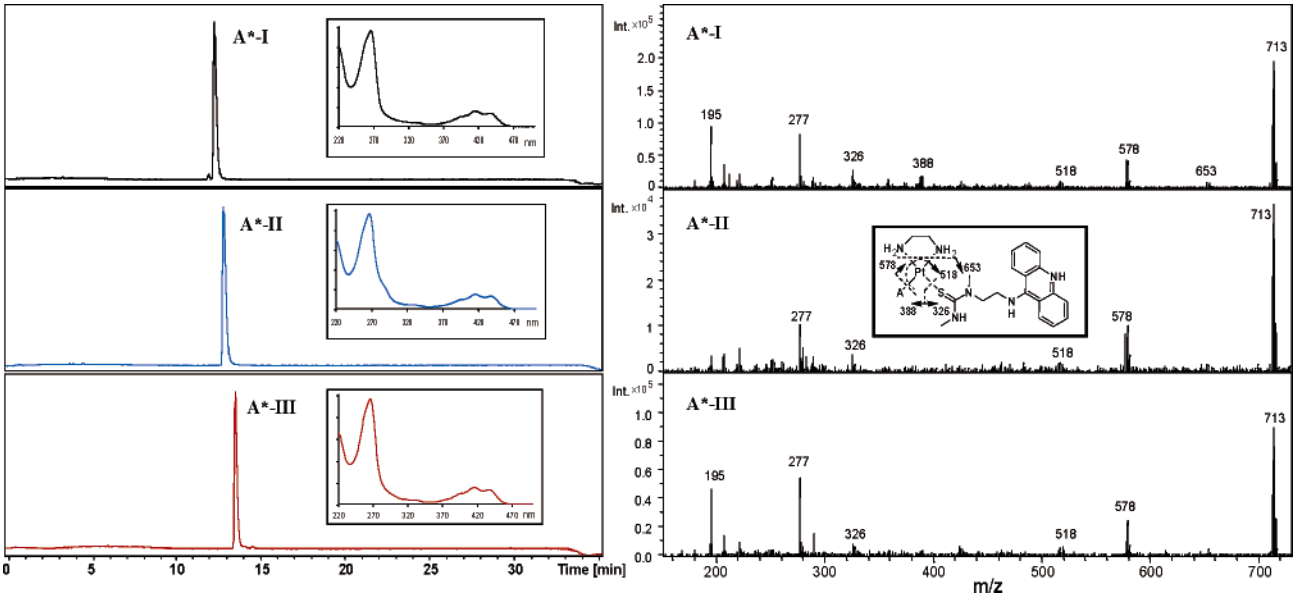

Figure 5. Characterization of **A*-I**, **A*-II**, and **A*-III** by in-line LC−MS. *Left*: HPLC traces of the isolated adducts, which elute at retention times of 12.4, 13.0, and 13.5 min. The insets show UV−visible traces for each adduct, confirming the presence of the acridine (370−470 nm) and adenine (266 nm) chromophores. Separations were done using HPLC protocol B; see Experimental Section. *Right*: Positive-ion electrospray mass spectra of the adducts showing peaks for the $[\mathbf{A^*\text{-}2H}]^+$ ions (*m*/*z* 713), and fragment ions resulting from in-source collisionally activated dissociation (CAD). Platinum-containing fragments show the characteristic Pt isotope pattern. The inset illustrates the common fragmentation pattern observed for the $[\mathbf{A^*\text{-}2H}]^+$ ions.

Chart 2

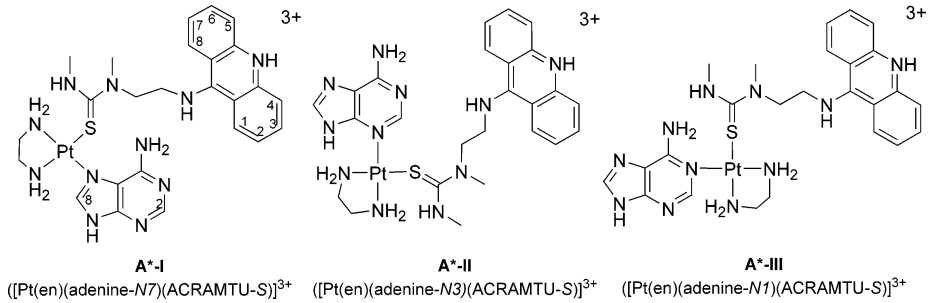

state (confirmed by tandem mass spectrometry and X-ray crystallography, vide infra).

A useful diagnostic tool in the assignment of linkage isomers of metalated nucleobases is the monitoring of the pH dependence of nonexchangeable base protons. Plots of $\delta_{H2/H8}$ versus pH (or pH* for D_2O solutions) show characteristic pK_a shifts for the proton-affinic ring nitrogens, which depend on the site of platination.[27,33] In addition, the magnitude of chemical shift differences, $\Delta\delta_{H2}$ and $\Delta\delta_{H8}$, between the protonated and unprotonated forms of the modified base gives information on the spatial proximity between H2/H8 and the protonation site.[27] The acid−base chemistry of platinum−adenine adducts has been investigated in great detail and can be summarized as follows.[21,27] Pt binding to N7 lowers the pK_a of N1. Inversely, Pt binding to N1 increases the basicity of N7. Similar to that of the N7-bound complexes, adenine-N3 binding has been reported to dramatically lower the pK_a of N1 while raising the pK_a of N7, ultimately reversing the order of basicity of the two endocyclic nitrogens relative to those in free adenine. For the free nucleobase, for example, in 9-methyladenine, pK_a values of −0.64 (N7) and 4.10 (N1) have been reported.[33] Adenine itself and adducts **A*-I**, **A*-II**, and **A*-III** contain another basic nitrogen, N9, which is usually not discussed because it is modified with an alkyl residue in DNA models to mimic the glycosidic base−deoxyribose linkage. A pK_a of 10.1, extracted from variable-pH ^{15}N NMR spectra, has been reported for this adenine nitrogen.[34] The plots of chemical shift versus pH*, shown in Figure 7, are in full agreement with the findings of previous studies of platinum-modified adenines. In addition to the characteristic pK_a shifts observed for N1 and N7, the distinct decrease in basicity of N9 proved to be useful for probing the linkage isomerism in the adducts. Platinum binding to N7 in adduct **A*-I** causes an acidification of N9 by approximately 4 orders of magnitude compared to that in free adenine, as evidenced by a drop in pK_a from ∼10 to ∼6.2. A similar, though less pronounced, effect on pK_a(N9) is observed for platination of N3 and N1 in **A*-II** and **A*-III**. N9 basicity appears to be least affected by platination of N1, which is located furthest from the monitored protonation site (for details, see caption of Figure 7). For comparison, pK_a(N9) values of 6.95 and 6.1 have been reported for N1- and N3-methylated adenine.[35] While the assignment of the pK_a values in adduct **A*-II** appears to be in agreement with those previously reported, one needs to bear in

(33) Kampf, G.; Kapinos, L. E.; Griesser, R.; Lippert, B.; Sigel, H. *J. Chem. Soc., Perkin Trans. 2* **2002**, 1320−1327.
(34) Gonnella, N. C.; Nakanishi, H.; Holtwick, J. B.; Horowitz, D. S.; Kanamori, K.; Leonard, N. J.; Roberts, J. D. *J. Am. Chem. Soc.* **1983**, *105*, 2050−2055.
(35) Stivers, J. T.; Jiang, Y. L. *Chem. Rev.* **2003**, *103*, 2729−2759.

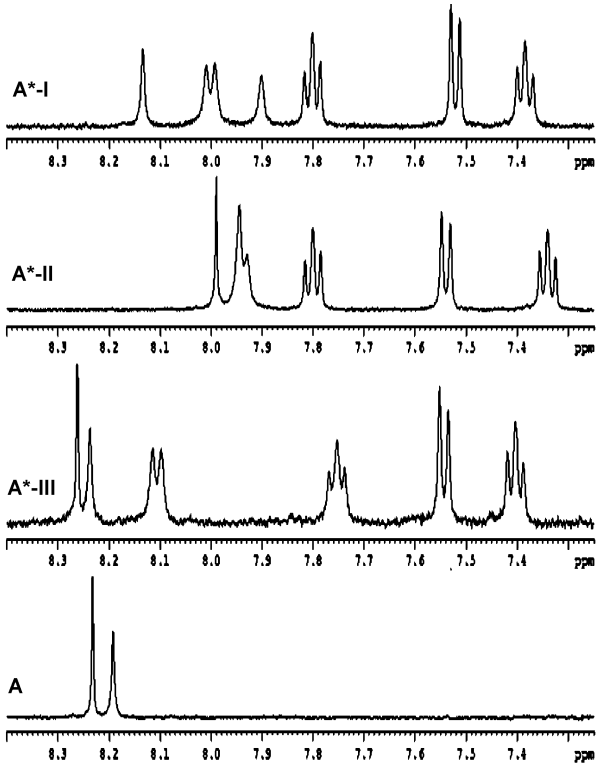

Figure 6. Stacked plot of the downfield regions in the ^{1}H NMR spectra (500 MHz, D_2O, pH* 6.2) of adducts **A*-I**, **A*-II**, **A*-III**, and free adenine base (**A**) showing aromatic acridine and nonexchangeable adenine protons. For signal assignments, see Table 2.

Table 2. ^{1}H Chemical Shifts[a] (500 MHz, 25 °C, D_2O, pH* 6.2) for Adducts **A*-I**, **A*-II**, **A*-III**, and Free Adenine Base (**A**)

		δ (mult)			
residue	proton	A	A*-I	A*-II	A*-III
adenine	H2	8.23 (s)	8.13 (s)	7.99 (s)	8.26 (s)
	H8	8.19 (s)	7.90 (s)	7.94 (s)	8.24 (s)
ACRAMTU	H1/H8		8.00 (d)	7.94 (d)	8.55 (d)
	H2/H7		7.38 (t)	7.34 (t)	7.40 (t)
	H3/H6		7.80 (t)	7.80 (t)	7.75 (t)
	H4/H5		7.52 (d)	7.54 (d)	7.54 (d)

[a] Assignments based on 2-D COSY, NOESY, and HMBC spectra and characteristic $^3J(^1H-^{195}Pt)$ couplings observed in 300 MHz ^{1}H NMR spectra, which resulted in broad unresolved platinum satellites for $H2_{Ade}$ and $H8_{Ade}$ (data not shown). Signals in the upfield region could not be assigned due to overlap with residual peaks of citrate ion introduced into the samples in the chromatographic separations.

mind that the majority of data was generated for N9-alkylated adenine derivatives. The binding of a positively charged complex to N3 of simple adenine lacking an N9 substituent, for instance, may change the N7-H/N9-H tautomeric equilibrium[34] of the nucleobase. While the N9-protonated form dominates in unmodified adenine, possibly due to elimination of repulsive interactions between the lone pairs on N9 and N3,[34] platination of N3 may shift the equilibrium toward the N7-protonated form. Thus, protonation of N7 and N9 of the nucleobase in **A*-II** (and in 3-methyladenine[35]) may actually occur in the reversed order compared to that proposed in Figure 7. This notion is further substantiated by the protonation state of adenine in the crystal structure of **A*-II**, which contains the adduct in its unexpected N7-protonated form (vide infra).

X-ray crystallographic data provided ultimate evidence for the proposed N3 coordination of the $[Pt(en)ACRAMTU]^{3+}$

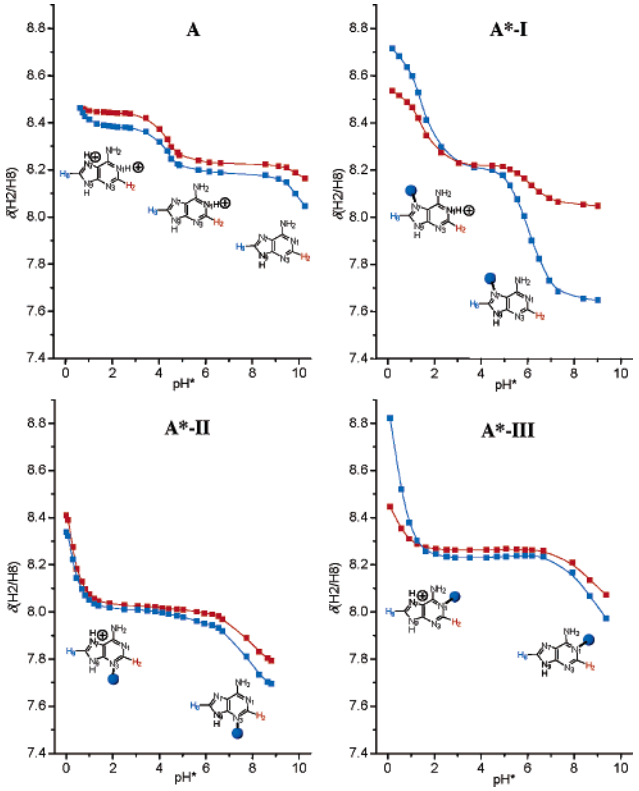

Figure 7. The pH dependence of $H2_{Ade}$ (red traces) and $H8_{Ade}$ (blue traces). ^{1}H chemical shifts in unmodified adenine (**A**) and the three platinum adducts, **A*-I**, **A*-II**, and **A*-III**. The maximum useful pH ranges were limited by compound solubility (pH* >9) and adduct decomposition (pH* <1). The structures show the proposed protonated state of each species at the respective pK_a. Blue spheres represent platinum. For **A*-I** and **A*-II**, biphasic curve fits could be performed, from which the following acidity constants were extracted: **A*-I**, pK_a(N1) ≈ 1.5, pK_a(N9) ≈ 6.2; **A*-II**, pK_a(N7) ≈ 0.4, pK_a(N9) ≈ 7.5. For alternate assignment of the pK_a values for **A*-II**, see the text. Assignments are based on the assumption that potential chemical shift changes for δ(adenine−H2/H8) resulting from deprotonation of the stacked ACRAMTU chromophores (pK_a ≈ 9.8; ref 11) at high pH are negligible.

fragment in adduct **A*-II**, the most striking DNA binding feature of PT-ACRAMTU. Suitable crystals of the adduct were grown by sitting drop evaporation. **A*-II** crystallizes in the triclinic space group $P\bar{1}$ as discrete $[(\mathbf{A^*\text{-}II})_2]^{6+}$ cations (Figure 8). $[(\mathbf{A^*\text{-}II})_2]^{6+}$ comprises a centrosymmetric dimeric entity, in which the adenine bases are mutually hydrogen-bonded through exocyclic NH_2 (N6) and endocyclic N1. The resulting A=A base pair is sandwiched between the acridine chromophores of the ACRAMTU ligands, which are stacked with the nucleobases at van der Waals distance. Another interesting feature in this structure is the protonation state of the platinated nucleobases, which exist in the less common N9-deprotonated/N7-protonated tautomeric form.[34] The proton on N7 was clearly identified in the difference Fourier map and shown to be involved in hydrogen bonding with a nearby water molecule in the crystal lattice.

Single crystals were also obtained of adduct **A*-I**. While the quality of the data set resulting from a weakly diffracting crystal did not allow a full (anisotropic) refinement of the structure, the preliminary structure (Supporting Information) unambiguously identifies **A*-I** as the proposed N7-linkage isomer. The data also indicate that this adduct forms pseudocentrosymmetric self-stacked dimers (space group $P2_1$), $[(\mathbf{A^*\text{-}I})_2]^{6+}$, similar to

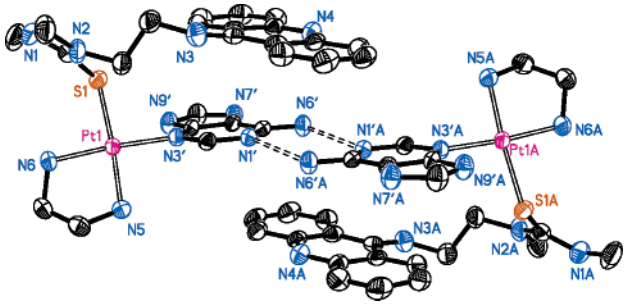

Figure 8. Thermal ellipsoid drawing of the centrosymmetric dimer $[(\mathbf{A^*\text{-}II})_2]^{6+}$ in the crystal with selected atoms labeled. To avoid ambiguities, the adenine nitrogen atoms in this scheme have been labeled with *primed* numbers. Hydrogen bonding within the A=A base pair is indicated by dashed lines. Hydrogens, counterions, and solvent molecules were omitted for clarity. Selected interatomic distances (Å) and bond angles (deg): Pt1−S1 2.308(1), Pt1−N3′ 2.037(3), Pt1−N5 2.066(4), Pt1−N6 2.032(4); S1−Pt1−N3′ 91.3(1), S1−Pt1−N6 92.6(1), N3′−Pt1−N5 92.7(1), N5−Pt1−N6 83.3(2), S1−Pt1−N5 175.5(1), N3′−Pt1−N6 175.3(1); N6′···N1′ (hydrogen bond donor−acceptor) 2.945(5) Å; the distance between average planes through acridine chromophores and the A=A base pair is 3.321 Å.

the N3 isomer. The only difference appears to be the interadenine hydrogen bonding, which in this case involves the N3 and (protonated) N9 positions of the nucleobases.

The type of self-association observed in **A*-I** and **A*-II** proves to be a common structural feature of nucleobases and nucleosides modified by PT-ACRAMTU. The stabilization of base pairing in the self-stacked dimeric structures by platinum−acridine, which has been observed previously in dGuo*,[19] provides a strong rationale for the coordinative−intercalative DNA binding mode of PT-ACRAMTU. NMR evidence, such as nuclear Overhauser effects and chemical shift anomalies, exists in the case of dGuo* that indicates the dimeric entity persists in solution and is not merely a crystal packing artifact.[19] Electrospray ionization mass spectra obtained for **A*-I** now confirm that this is also the case in the platinum−adenine system; in spectra acquired in positive-ion mode (Figure 9a), a low-intensity peak is observed at *m*/*z* 1425 for the $[(\mathbf{A^*\text{-}I})_2-5\mathrm{H}]^+$ ion, indicating that a minor fraction of the adduct exists as dimers in the gas phase, along with the monomer (*m*/*z* 713) and the fragment ions discussed earlier. Tandem MS/MS analysis of the *m*/*z* 1425 ion under mild conditions using collision-induced dissociation (CID) resulted in a fragmentation pattern dominated by characteristic fragment ions originating from the dimer (Figure 9b). Two major fragments are observed resulting from dissociation of a single ACRAMTU ligand (*m*/*z* 1100) and loss of a single adenine (*m*/*z* 1290). In contrast, in these spectra, the monomeric ion, $[\mathbf{A^*\text{-}I}-2\mathrm{H}]^+$, is completely absent. These data confirm the unusual stability of the dimeric entity resulting from the combined, and potentially synergistic, effects of nucleobase−nucleobase hydrogen bonding and acridine−base pair stacking.

Discussion

PT-ACRAMTU is the first platinum-based complex that recognizes and binds to minor-groove adenine-N3 in biologically relevant DNA. The formation of **A*-II**, which is virtually absent in single-stranded DNA, obviously requires a double-stranded template directing platinum into the minor groove. (Intercalation of ACRAMTU has been confirmed by NMR spectroscopy to occur from the minor groove.[16]) In contrast, the molecular recognition between cisplatin and DNA is dominated by the associative substitution chemistry of platinum with guanine-N7, which is kinetically and thermodynamically favored over adenine-N7 binding. A recent theoretical study[36] concludes that both the better donor ability of the guanine-N7 lone pair and the stronger hydrogen bonding in a pentacoordinated transition state contribute to the well-established nucleobase preference of cisplatin. The formation of only a minor fraction of 1,2 intrastrand A-N7/G-N7 cross-links in random-sequence DNA mirrors the reduced affinity of this drug for adenine-N7.[37] Adduct formation of platinum with adenine involving endocyclic nitrogens other than N7 is virtually unknown in native double-stranded DNA. Binding to N3, for instance, can only be artificially induced by disfavoring N7 and N1 binding in suitably modified bases.[21,22] Recently, an unusual A-N3-containing cross-link has been reported for a transplatinum complex in a dinucleotide sequence.[20] The model reaction studied produces a G-N7 monofunctional adduct, which subsequently closes to form an A-N3/G-N7 chelate similar to the A-N7/G-N7 cross-link. This is different from monofunctional PT-ACRAMTU, which *genuinely targets adenine-N3* without requiring prior reaction with an adjacent guanine base.

In light of the computational study,[36] it appears that cisplatin's lack of adenine-N3 affinity is most likely a consequence of steric factors (presence of a bulky deoxyribose residue on N9) as well as an absence of transition state stabilizing hydrogen bonding. Unlike platinum, several minor-groove-oriented DNA alkylating agents modify adenine at N3, and many oligoamides, natural and synthetic, recognize this site through hydrogen bonding.[38] Inspired by the DNA interactions of these agents, the *cis*-diaminedichloroplatinum(II) moiety has been tethered to distamycin,[39,40] a minor-groove-binding agent with a distinct preference for AT-rich DNA sequences.[41] It was hoped that this conjugation would change the sequence and groove specificity of platinum. In platinum−distamycin, however, the metal dominates the base and groove specificity, resulting in an array of cross-links similar to those observed for nontargeted cisplatin.[39] Another interesting observation has been reported recently for the trinuclear platinum drug BBR3464. NMR evidence was presented[42] suggesting that the DNA binding mechanism involves preassociation of the complex with the minor groove. However, in this case, multiple pathways exist allowing the platinum moieties to diffuse into the major groove, ultimately resulting in long-range cross-links with guanine-N7 positions.

The unique DNA recognition by PT-ACRAMTU leads to the promiscuous targeting of guanine (N7) and adenine (N1, N3, N7) nucleophilic sites at the base-pair steps into which the conjugate (pre)intercalates. In previous work, we have speculated that PT-ACRAMTU might target the minor groove of DNA based on the DNA interactions of unmodified ACRAMTU[16] and restriction enzyme DNA cleavage experiments performed for the conjugate.[18] We have now demonstrated that platination of adenine-N3, in fact, occurs in a template-specific manner.

(36) Baik, M.-H.; Friesner, R. A.; Lippard, S. J. *J. Am. Chem. Soc.* **2003**, *125*, 14082−14092.
(37) Fichtinger-Schepman, A. M. J.; van der Veer, J. L.; den Hartog, J. H. J.; Lohman, P. H. M.; Reedijk, J. *Biochemistry* **1985**, *24*, 707−713.
(38) Yang, X.-L.; Wang, A. H.-J. *Pharmacol. Ther.* **1999**, *83*, 181−215.
(39) Loskotova, H.; Brabec, V. *Eur. J. Biochem.* **1999**, *266*, 392−402.
(40) Kostrhunova, H.; Brabec, V. *Biochemistry* **2000**, *39*, 12639−12649.
(41) Iida, H.; Jia, G. F.; Lown, J. W. *Curr. Opin. Biotechnol.* **1999**, *10*, 29−33.
(42) Hegmans, A.; Berners-Price, S. J.; Davies, M. S.; Thomas, D. S.; Humphreys, A. S.; Farrell, N. *J. Am. Chem. Soc.* **2004**, *126*, 2166−2180.

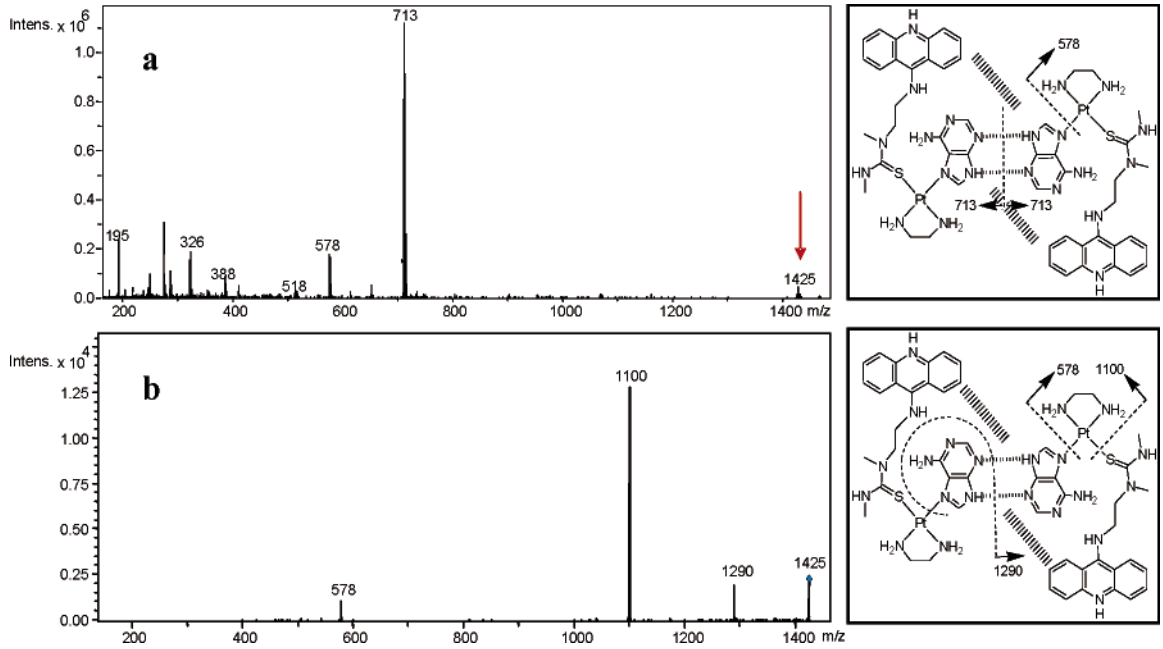

Figure 9. Positive-ion electrospray mass spectrum (a) and tandem (MS^2) mass spectrum (b) of adduct **A*-I** with schemes illustrating the distinct fragmentation of the dimer in each experiment. *Hashed* lines were used to indicate interbase hydrogen bonding and base stacking.

The adenine adduct profiles established in $d(TA)_5$, $d(TA)_{15}$, and calf thymus DNA demonstrate that even though major-groove binding cannot be abolished, minor-groove adduction is enhanced with increasing thermal stability of the duplex (10mer < 30mer < native DNA). The opposite is true for binding to the N1 site, which becomes less accessible in double-stranded DNA. One potential mechanism of DNA binding of PT-ACRAMTU involves rapid intercalation of the planar chromophore from the minor groove, followed by platination of nitrogen at the intercalation site. Thus, the relative yields of the N1, N3, and N7 adducts can be expected to be sensitive to dynamic effects, such as on/off rates of the preintercalated complex as well as base-pair opening rates and deformability of the target duplex.[43,44] To prove this supposition and to find a correlation between adduct distribution and biological activity, current work in our laboratory is concerned with the design of PT-ACRAMTU analogues exhibiting enhanced adenine-N3 specificity. Logically, this could be achieved by tuning the overall AT affinity of the conjugate and by increasing the residence time in the minor groove of the preintercalated drug. Chemical modifications are also being made that should prevent the platinum moiety from threading the duplex, thereby reducing purine-N7 binding in the major groove.

PT-ACRAMTU forms adducts with purine bases in both grooves of the biopolymer, all of which have to be considered potential cytotoxic lesions. In particular, the biological consequences of minor-groove adducts of PT-ACRAMTU are potentially serious. The ideal coplanar stacking of the acridine chromophores with the A=A base pair in the crystal structure of **A*-II** (Figure 8) suggests that the combined coordinative binding of platinum and intercalation of acridine into the DNA base stack from the minor groove might be a feasible binding mode in double-stranded DNA. To address this issue and to explore the structural factors that might favor, or disfavor, minor-groove adducts of this type of conjugate, a future NMR/modeling study will be performed on a site-specifically modified model duplex containing adduct **A*-II**. TA-rich sequences are the sites of transcription initiation ("TATA boxes") for type II eukaryotic genes.[45] TATA binding proteins (TBP) associate with DNA through the minor groove,[46,47] which is an important signaling event in the assembly of the RNA polymerase II holoenzyme complex. Blocking of TBP binding sites by bulky minor-groove adducts of PT-ACRAMTU could lead to faulty or incomplete transcription of genetic information, a potentially cytotoxic event. Sequences of high AT content might be another promising target for PT-ACRAMTU and its improved analogues. Recently, several hypercytotoxic minor-groove binders have been discovered belonging to the class of cyclopropylpyrroloindoles, which specifically alkylate adenine-N3 within certain domains of the human genome referred to as AT islands.[48] AT islands play a critical role in replication. Expanding the repertoire of AT island targeted agents to platinum-containing drugs appears to be an attractive opportunity in anticancer drug development.

Acknowledgment. This work was supported by the National Institutes of Health/National Cancer Institute (Grant R01-CA101880) and the North Carolina Biotechnology Center (Grant 2001-ARG-0010). The collection of CCD X-ray data and LC−MS measurements were performed on instruments purchased with funds provided by the National Science Foundation (Grant CHE-0234489) and the North Carolina Biotechnology Center (Grant 2001-IDG-1004). We thank one of the reviewers for his/her helpful comments on the assignment of the pK_a

(43) Guéron, M.; Leroy, J.-L. *Methods Enzymol.* **1995**, *261*, 383−413.
(44) Lankas, F.; Sponer, J.; Langowski, J.; Cheatham, T. E. *J. Am. Chem. Soc.* **2004**, *126*, 4124−4125.
(45) Horton, H. R.; Moran, L. A.; Ochs, R. S.; Rawn, J. D.; Scrimgeour, K. G. *Principles of Biochemistry*; Prentice Hall: Upper Saddle River, NJ, 2002; Chapter 21.
(46) Jou, Z. S.; Chiu, T. K.; Leiberman, P. M.; Baikalov, I.; Berk, A. J.; Dickerson, R. E. *J. Mol. Biol.* **1996**, *261*, 239−254.
(47) Morávek, Z.; Neidle, S.; Schneider, B. *Nucleic Acids Res.* **2002**, *30*, 1182−1191.
(48) Woynarowski, J. M.; Trevino, A. V.; Rodriguez, K. A.; Hardies, S. C.; Benham, C. J. *J. Biol. Chem.* **2001**, *276*, 40555−40566.

values. A generous loan of potassium tetrachloroplatinate(II) from Johnson Matthey PLC (Reading, U.K.) is gratefully acknowledged.

Supporting Information Available: Thermal melting curves and CD spectra of the synthetic oligonucleotides (Figure S1) and experimental details of the measurements; details of the X-ray structure determinations of [(**A*-I**)]$(NO_3)_3 \cdot 4H_2O$ and [(**A*-II**)]$(NO_3)_3 \cdot 5H_2O$ in CIF format; crystal data for [(**A*-I**)]$(NO_3)_3 \cdot 4H_2O$ (Table S1) and the view of the $[(\mathbf{A^*\text{-}I})_2]^{6+}$ ion in the crystal (Figure S2). This material is available free of charge via the Internet at http://pubs.acs.org.

JA0451620